Further Characteristic Analysis of theHigh-Power AC Plasmatron

Sedanur Toraman[1], T. Y. Katırcıoğlu[2]

[1]Msc. Metallurgical and Materials Engineering, ARTECS Anadolu R&D Technology Engineering and Consultancy Inc. BahçelievlerMahallesi Ankara ÜniversitesiTeknokentBinası D Blok No:7 06830 Gölbaşı Ankara
[2]PhD., Chemistry, ARTECS Anadolu R&D Technology Engineering and Consultancy Inc.
Corresponding Author: T. Y. Katırcıoğlu

ABSTRACT: *With our previous publication, characterization of the high-power arc-jet plasma torch was studied. This article attempts to carry out further characterization of the plasma jet using different experimentalresults mainly obtained from different distances ofoptical emission spectroscopy (OES) and different arc power values. Plasmatron works under atmospheric (about one atm) pressure with high-power three phase alternating-current (AC) established in AR&TeCS (ARTECS Anadolu R&D Technology Engineering and Consultancy Company, Ankara University Technopolis). In order to characterize the plasma, the electron temperature (T_e) and electron density (n_e) were determined by using OES in the range $200 – 1100$ nm as defined in the experiment section. In this study, the measured emission spectra and identification of spectrum lines were evaluated and T_e and n_e were calculated according to different distances of OES and different arc power values. The strongest NII lines (nitrogen atomic lines) was observed at 510.44 nm with the transition of $2s^22p3p\ ^1S$ - $2s^22p4s\ ^1P^0$. The other NII lines were observed at 589.32 with the transition of $2s2p^2(^4P)3s\ ^3P$ - $2s2p^2(^4P)3p\ ^3D^0$, at 606.67 nm with the transition of $2s^22p3p\ ^3P$ - $2s^22p3d\ ^1D^0$ and at 616.8 nm with the transition of $2s^22p3d\ ^3F^0$ - $2s^22p4P\ ^3D$. The T_e was calculated in the range of 11248 - 12870 K by means of local thermodynamic equilibrium model. The n_e was calculated with respect to the McWhirter criterion and it was between $2.429\times10^{21}\ m^{-3}$ and $2.587\times10^{21}\ m^{-3}$. It was seen that the T_e and n_e were found at the expected levels compared with similar studies in the literature. In addition to OES method, the other methods employed for the evaluation of plasma parameters were described briefly in this paper. Moreover, the calorimetric heat flux probe was used in this study to measure and characterize the plasma and the chamber temperature was calculated by using Gas Dynamic Method. The average values obtained in the range of 664.8 – 1133.1 kW power levels from experiments are given as following: the plasma torch chamber temperature around 4000 K and the heat flux above 2.61 MW/m^2.*
Keywords: Plasma diagnostic, Atmospheric plasma, OES, Electron temperature,Electron density

----

I.   INTRODUCTION

Plasma which is referred as the fourth state of matter composes more than 99% of the universe. It is an ionized gas and consists of electrons, positive and negative ions and neutral species [1]. Plasmatron is an electro-technology device that converts electrical energy into thermal energy. Plasmatrons have a wide range of applications and usage area due to the very high level of temperature which they can reach. They are used widely in aerospace technologies, energy, metallurgy, surface coatings, chemical synthesis, machining, medicine, textile, thermochemical processes like gasification and combustion processes [2].

Plasmas can be divided into thermal plasma (high temperature) and cold plasma (low temperature) according to their working power. Also, thermal plasma and cold plasma are referred as plasmas which are in local thermal equilibrium and which are not in local thermal equilibrium, respectively. The local thermal equilibrium (LTE) means that the temperature of all plasma species such as electrons, ions, neutral particles is the same in a localized area in the plasma. On the other hand, the non-local thermal equilibrium (non-LTE) implies that the temperature of the different plasma species is not same [3-4]. Various plasma parameters such as electron density (n_e) and electron temperature (T_e) are essential to obtain information about the characteristics of the plasma. While LTE plasmas have high electron density ($10^{21} – 10^{26}\ m^{-3}$), electron density is low ($< 10^{19}\ m^{-3}$) in non-LTE plasmas [1]. The electron temperature is close to the heavy particles temperature for LTE plasmas. For example, in an arc plasma (core) ($T_e = T_h \approx 10000$ K). However, for non-LTE plasmas, the electron temperature is much higher than the temperatures of heavy particles like ions, atoms, molecules ($T_e \gg T_h$). To give an example, in glow discharges $T_e \approx 10000 – 100000$ K and $T_h \approx 300 – 1000$ K [5]. The range of plasma

parameters are given inFigure 1as (n, T) plot [6]. According toFigure 1, our plasma represents the thermal processing plasmas region and the experiment results show that the electron temperature and electron density are envisaged approximately 12149 K and 2.515×10^{15} cm^{-3}, respectively.
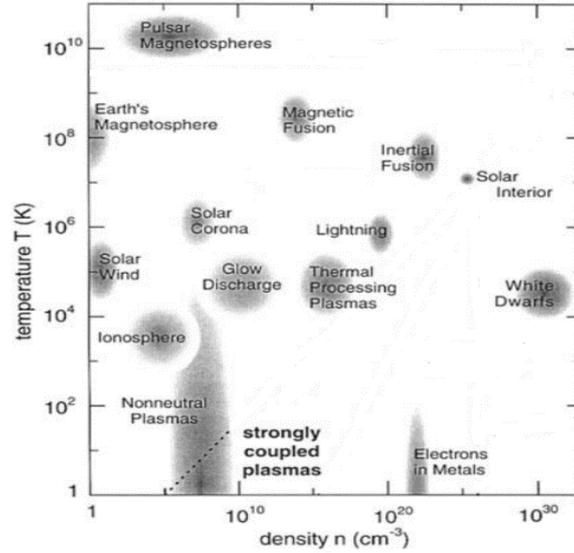

Figure 1: Range of plasma parameters.

Many different techniques are being employed to measure and evaluate various plasma parameters such as electron temperature, ion and electron densities, electron distribution function, chemical compositions and species of the plasma, plasma potential, etc. [7]. Probes, magnetics, mass spectroscopy, microwave diagnostics, particle diagnostics and optical emission spectroscopy (OES) are among these techniques which are shortly introduced in the following sections [8].

Probes are in direct contact with the plasma and the Langmuir probe is the most well-known and used. The electron temperature, electron density, plasma potential and electron and ion beam energy over an extremely wide range of parameters can be determined by Langmuir probe which measure the current to the probe as a function of the difference between the probe and plasma space potentials [9-10]. **Magnetics** are utilised the electromagnetic waves emitted by the plasma to measure the plasma current, position, shape, pressure and also detect plasma instabilities. **Mass spectroscopy** ionizes chemical species and organizes ions according to their mass-charge ratios. Moreover, it widely used in space missions to measure the composition of plasmas and plasma − surface interactions [9]. **Microwave diagnostics** can be categorised as interferometry, electron cyclotron emission (ECE) and absorption (ECA) and Thomson scattering. The phase shift of the microwaves transmitted through the plasma is determined and the average electron density is concluded from the amount of phase shift by using interferometry [10]. ECE measures the electron temperature and its fluctuations while ECA can measure the electron pressure [11]. The Thomson scattering method can be used to measure the velocity distribution of fast ions or the electron density [12]. **Particle diagnostics** can be classified as neutral particle analysis (NPA) and charge exchange recombination spectroscopy (CXRS). NPA can diagnose the temperature of hydrogenic ion species in the plasma core at higher energies. CXRS can be used to obtain information on the ion temperature, ion density, ion rotation, electron density fluctuations and internal magnetic field. **Optical emission spectroscopy (OES)** is the most important and frequently used plasma diagnostic since it is least perturbative method. Moreover, OES which characterize the plasma parameters at wide temperature and pressure ranges can be used as a control tool that enables time and spatial monitoring of the plasma during the process [7,13]. In atmospheric thermal plasmas, local thermal equilibrium conditions are applicable since high pressure causes an increase in collisions and then the electrons assign their energies to the other heavy particles. Thus, the electron temperature is close to gas temperature [14].

Local Thermal Equilibrium (LTE)

In the LTE concept, Boltzmann and Saha equations which govern the electron distribution function is assumed to be Maxwellian at each point in the plasma according to the electronic temperature [15]. The collisions with electrons are dominant in the radiative processes, which results in the existence of sufficiently high electron density [16]. For that matter, a criterion proposed by McWhirter was based on the existence of a critical electron density [17]:

$$n_e \geq 1.6 \times 10^{12} (T)^{1/2} (\Delta E)^3 \tag{1}$$

In Equation (1), n_e (cm^{-3}), T (K) and ΔE (eV) refers to the electron density, the plasma temperature and the energy gap respectively. The critical electron density values are typically in the range $10^{15} - 10^{16}$ cm^{-3} [16]. In study of an example of atmospheric pressure air plasma in LTE, the electron temperature is about 1 eV and the electron density is calculated as 1.0×10^{21} m^{-3} [18]. In this study, the value of electron density is determined by means of the Equation (1).

Maxwell Distribution:

According to the Maxwell's law, the distribution of the particles constitutes the plasma with respect to their velocities. The density, dN, of any particles with velocities in the $v + dv$ range can be described as $dN = Nf(v)dv$, where N is the density of the particles and $f(v)$ is the Maxwell velocities distribution function [7]:

$$f(v) = 4\pi r^2 \left(\frac{m}{2\pi kT}\right)^{3/2} \exp\left(-\frac{mv^2}{2kT}\right) \tag{2}$$

where k is the Boltzmann's constant (1.38×10^{-23} J/K), m is the mass of the particle and T is the temperature [19].

The number of the free electrons with velocity in the range $(v_e + dv_e)$ is:

$$dn_e = 4\pi n_e \left(\frac{m}{2\pi kT_e}\right)^{3/2} \exp\left(-\frac{mv_e^2}{2kT_e}\right) v_e^2 dv_e \tag{3}$$

where n_e is the total electron density, T_e is the electrons temperature, k is the Boltzmann's constant and m is the electron mass [20].

II. METHOD

In this work, the electron temperature and electron density were determined by using OES method which provides the ability to obtain data by measuring the properties of the light on the electromagnetic spectrum that the materials transmitting. Because of collisions between particles and free electrons in the plasma, particles are excited to rise from low energy to high energy level. The excited electrons go back to low energy level since they are not stable in this case. At the same time, they emit photon by converting their heat energy to electromagnetic energy. The energy of emitted photon is equal to the difference between higher (E_2) and lower (E_1) energy state and corresponding with wavelength of spectral line described by following equation [21]:

$$\lambda = \frac{hc}{E_2 - E_1} \tag{4}$$

where h is Planck's constant which has a value of 6.6261×10^{-34} m^{2}kg/s, c is the speed of light, E_2 and E_1 is excited and lower energy state, respectively. The electron temperature is calculated from Boltzmann plot as detailed in the "Results and Discussion" part.

With the optical emission spectrometer, the light from the plasma stream is collected by a fibber optic spectrometer into the digital medium as an intensity - wavelength graph and the plasma parameters such as electron temperature, electron density can be reached by graphical analysis. Because this method does not interfere with the plasma, it is possible to measure it without deterioration of the plasma.

OtherPerformance Measurements:
Heat Flux Measurement

While OES gives information about plasma parameters such as electron temperature, electron density, particle composition; specific probes like heat flux probes give much-needed information about the plasma flow. The heat flux probe which can be used to determine the local enthalpy is calculated by following equation [22].

$$qS = \dot{m}c_P(T_{out} - T_{in}) \tag{5}$$

where q is the stagnation-point convection heat flux rate, S is surface area of the probe, $\dot{m}$ is the mass flow rate of the water and c_p is the specific heat of the water, T_{in} is the temperature of the inlet water to the cooling surface of the copper surface and T_{out} is the temperature of the water coming out of the cooling surface of the copper surface. The left side demonstrates power brought from the plasma jet into the probe and the right side shows power evacuated by the cooling circuit of the probe [2].

Chamber Temperature Calculation via Gas Dynamic Method

The most important electrical characteristics of the plasma torch is the Volt-Ampere Characteristics (VAC) [22]. According to [23], the independent parameters are given as: I^2/Gd, G/d, pd, BI/pd, I^2/pd^2 and so on. Also, the dependent parameters are defined as: U, Ed, Ud/I, Ed^2/I, η and so on.

Equation (6) gives the gas flow rate which is calculated by measuring a pressure difference of the venture nozzle and temperature of the gas in gas collector just before entering the plasma system.

$$G_g = \frac{m \cdot P_w \cdot F_w \cdot q_l}{\sqrt{T_g}} \tag{6}$$

where m is a constant value (0.3965), P_w is the pressure of venture, F_w is area of the venture ($F_w = d_w^2 \cdot \frac{\pi}{4}$), q_l is also a constant value equal to 1 and T_g is the temperature (288 K) [23]. Here, the error due to the cold gas temperature change can be neglected because the methodological error is very small.

Furthermore, the chamber temperature is calculated by using Gas Dynamic Method. According to this method, the following analysis method is coded in the software:

$$f(T_{ch}) = G_g/F_{noz} \cdot P_{ch} \tag{7}$$

Here, f is a function of chamber temperature, G_g is the gas flow rate, F_{noz} is the cross-sectional area of nozzle and P_{ch} is the chamber pressure which is measured directly using pressure transducer. As seen in Equation (7), the chamber temperature is directly proportional to the gas flow rate and the chamber pressure since the cross-sectional area of nozzle has a constant value.

III. EXPERIMENTAL SET-UP

In this work, results of two plasma parameters (the electron temperature and the electron density) are presented with respect to different arc powers and distance. For this purpose, the air plasma investigated in AR&TeCS facility is produced with a high-power AC three-phase plasma torch. In Figure 2, the plasma torch which has been designed at Keldysh Research Center (KeRC) is shown schematically. This type plasma torch includes the mutual mixing chamber (1) and three identical arc chambers. Each of them consists of the back plate (2), the electrode (3) and the constrictor (4). The back plate and the constrictor are separated by electrical insulators in which the working gas (air) is supplied to produce a vortex. Moreover, each electrode is fitted with solenoids and the magnetic of solenoids results in a rotation of the radial part of the arc [2]. The plasma torch system consists of five subsystems which are electrical subsystem, cooling subsystem, gas feeding subsystem, ventilation subsystem and data acquisition (DAQ) and control subsystem.
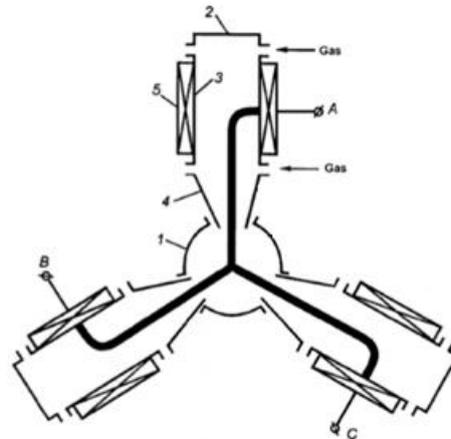

Figure 2: The schematic diagram of the AC three-phase plasma torch [23].

The experimental data presented in this study were obtained using OES which is placed and studied at the AR&TeCS facility. Figure 3shows a schematic of the experimental set-up for OES measurements.
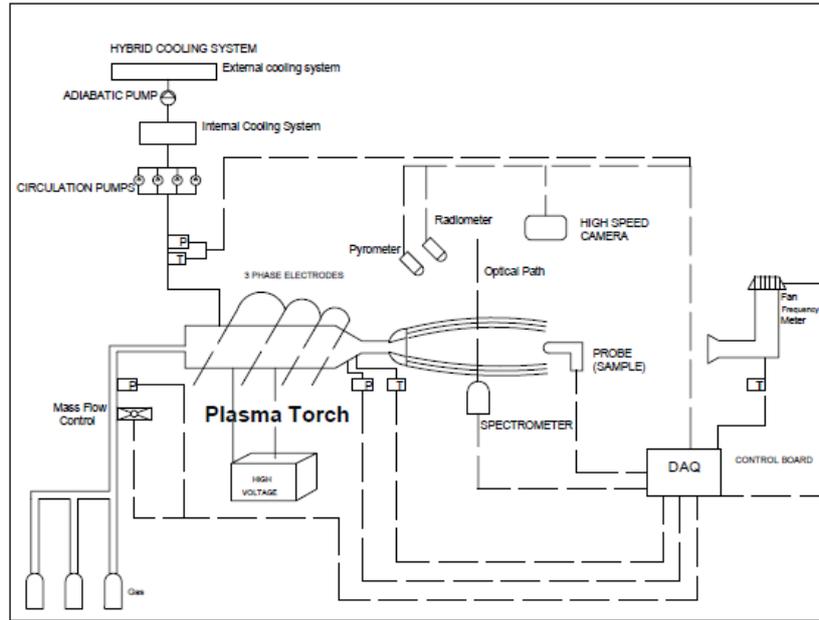
Figure 3: The schematic of the experimental set-up.

The optical emission spectrum is obtained with the Ocean Optics HR-4000-UV-NIR model spectrometer, which can measure at 200-1100 nm wavelength range from the plasma flow at the plasma torch nozzle outlet. The optical spectrometer has a composite grating capable of measuring within the range of about 200-1100 nm. Plasma spectroscopy uses the HR4000, a detector with a low slit spacing and a large number of pixels. The connection between the spectrometer and the computer is provided by means of a USB cable. The COL UV lens with a focal length of 30 mm collects light at an angle close to 180°. The optical spectrometer was placed at different distances and measurements were made.

IV. RESULTS AND DISCUSSION

The different methods are used in the literature for different plasma species at spectroscopic analysis. When atmospheric plasmas are evaluated, collisions in atmospheric plasmas are more dominant and local thermodynamic equilibrium is approached. Therefore, LTE model is used for the electron temperature and the electron density in this study. O, N, N_2, O_2, CO, NO and OH radicals are observed in measurements with optical emission spectrometer from high power AC plasma torch operating with air as working gas at ARTECS facility. The most abundant (78%) element is Nitrogen in the air. Thus, experimental calculations of plasma parameters were done with respect to NII- singly ionized emission atomic lines. According to the LTE model, the temperature of the arc plasma gas (the electron temperature) is calculated by Equation 8 [24].

$$\ln\left[\frac{I_2\lambda_2}{g_2A_2}\right] = -\frac{E_2}{kT} + c \tag{8}$$

I_2, λ_2, g_2, A_2, E_2, k and T in this equilibrium are the high level intensity of light, the high level wavelength, the statistical weight, the Einstein transition probability, the high energy level, the Boltzmann constant and the excitation temperature, respectively. Also, c is a constant. While the values of g_2, A_2 and E_2 are obtained from the National Institute of Standards and Technology [25], the values of I_2 and λ_2 are obtained from OES spectrum. $\ln\left[\frac{I_2\lambda_2}{g_2A_2}\right]$ versus E_2 plot gives a straight line with a slope of $-1/kT$ and the electron temperature can be determined. Moreover, the electron density can be calculated according to the McWhirter criterion by Equation 1 ($n_e \geq 1.6 \times 10^{12} (T)^{1/2} (\Delta E)^3$) given in Introduction section.

During the experiment, the arc voltage and current are measured using a standard type of network analyser. Before the experiment, the impedance value at the desired stage, that is, the current value is adjusted with the current limiting reactors for each phase. It can be seen that there is a maximum 2 % error when this current value is compared with the average current value measured during the experiment. In Figure 4 andFigure 5, the graphs of voltage-time and current-time are given, respectively. It can be seen from these graphs that the current values are stable being independent parameters around adjusted values; however, the voltage is not stable because it is a dependent parameter of plasma torch working conditions. Also, the electric power used by plasma was calculated using voltage and current values from the following equation.

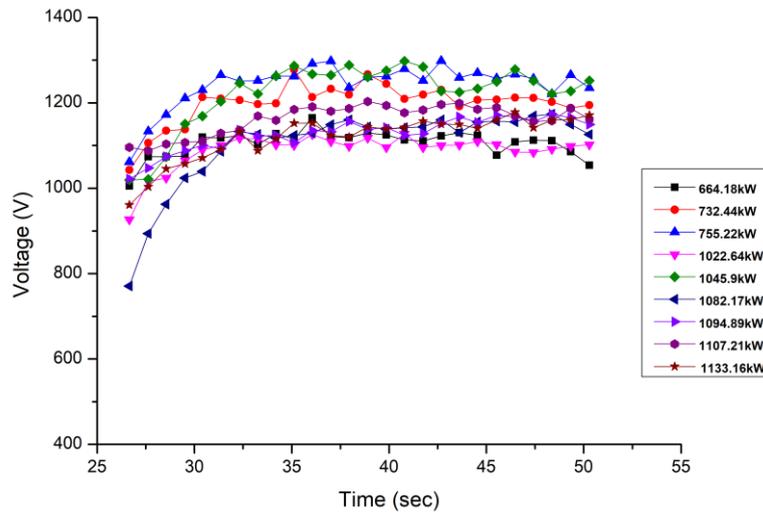$$P = U_1 \cdot I_1 + U_2 \cdot I_2 + U_3 \cdot I_3 \tag{9}$$

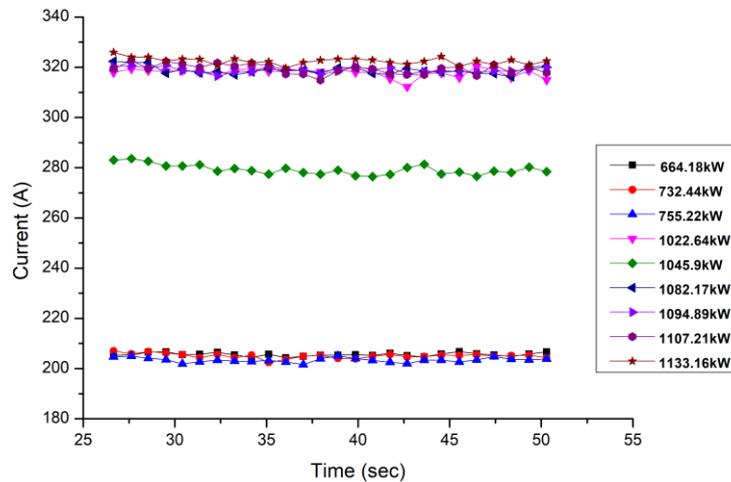**Figure 4: The graph of voltage versus time for many experiments.**

Figure 5: The graph of current versus time for many experiments.

An example of OES spectrum of the plasma is given inFigure 6. The detailed OES spectrums of the plasma are also observed with respect to the power in this figure. In this experiment, the spectrometer was positioned 53.5 cm away from the plasma flow and receiving data from the firs 5.5 cm of the flow. As seen inFigure 6, the most intense peak at the visible range belongs to the NII atom at 510.44 nm. Moreover, the spectral emission lines of NII are listed in Table 1for Boltzmann plot to determine the plasma electron temperature and the electron density.
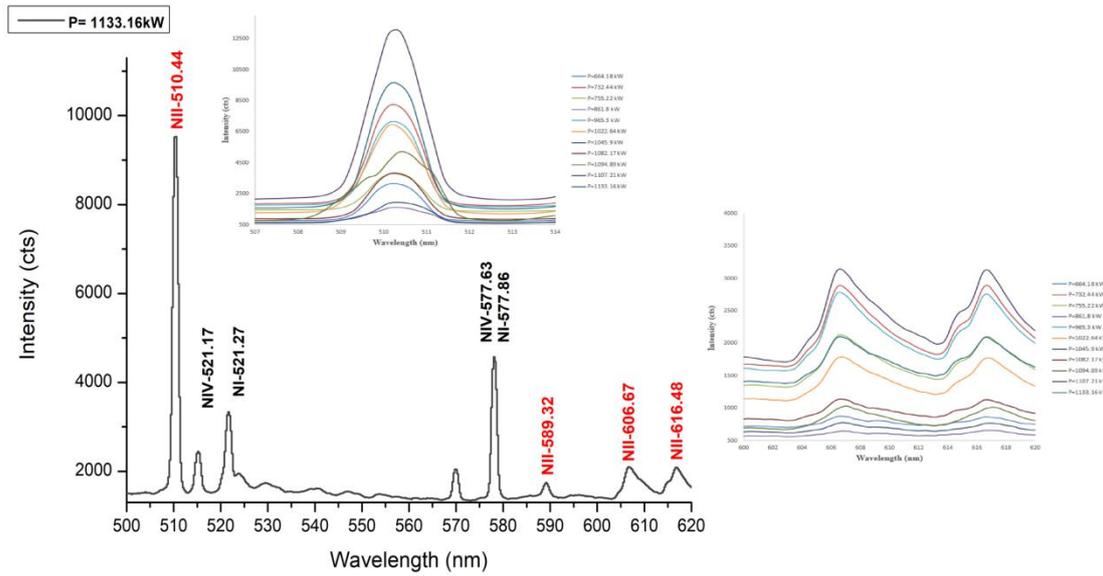
Figure 6: The emission spectrum of arc plasma at P=1133.16 kW with the power evolutions of specified NII peaks.

Table 1:Spectral atomic line parameters of singly ionized nitrogen-NII

Wavelength (nm)	g_2A_2 (s^{-1})	E_1 (cm^{-1})	E_2 (cm^{-1})	Lower Level Configuration	Upper Level Configuration	Intensity (cts)
510.44	3.03E+07	178273.38	197858.69	$2s^22p3p\ ^1S$	$2s^22p4s\ ^1P^0$	9530.44
589.32	2.02E+08	211827.67	228791.83	$2s2p^2(^4P)3s\ ^3P$	$2s2p^2(^4P)3p\ ^3D^0$	1745.72
606.67	1.28E+06	170607.89	187091.37	$2s^22p3p\ ^3P$	$2s^22p3d\ ^1D^0$	2097.16
616.8	1.86E+08	186652.49	202861.36	$2s^22p3d\ ^3F^0$	$2s^22p4P\ ^3D$	2088.68

InFigure 7, the Boltzmann plot is given for the power 1133.16 kW. The electron temperature is calculated as 12063 K (~ 1 eV) and the electron temperature is estimated as 2.51×10^{21} m^{-3}.
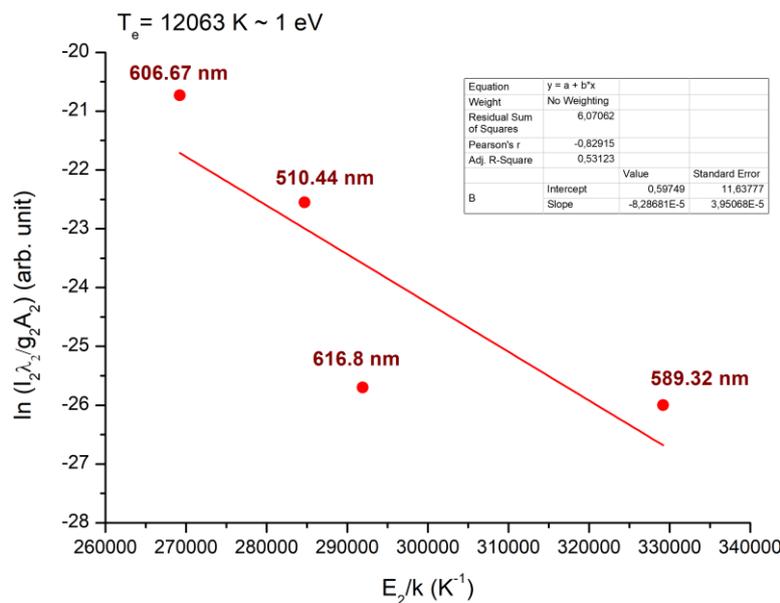

Figure 7: Linear Boltzmann plot of the NII peaks to estimate the electron temperature.

Figure 8and Figure 9 represent the arc plasma power dependence of T_e and n_e, respectively. The spectrometer was positioned 53.5 cm away from the plasma flow and data were received from the first 5.5 cm of

the flow. As it seen from these figures that the range of the electron temperature changes from 11376 K to 12870 K and the electron density changes from 2.440×1021 m^{-3} to 2.598×1021 m^{-3} while the power changes from 750 kW to 1100 kW. These results show that the electron temperature and the electron density increase up to 1050 kW since first free electrons gain more energy as a result of the collisions. Then, the both parameters decrease because the electrons transfer their energy to the other particles (ions and neutrals).
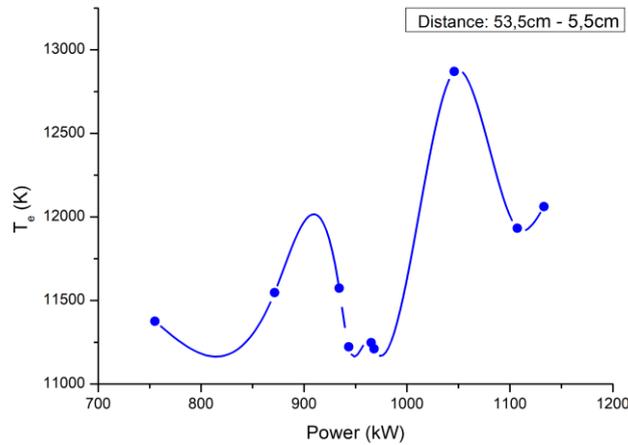

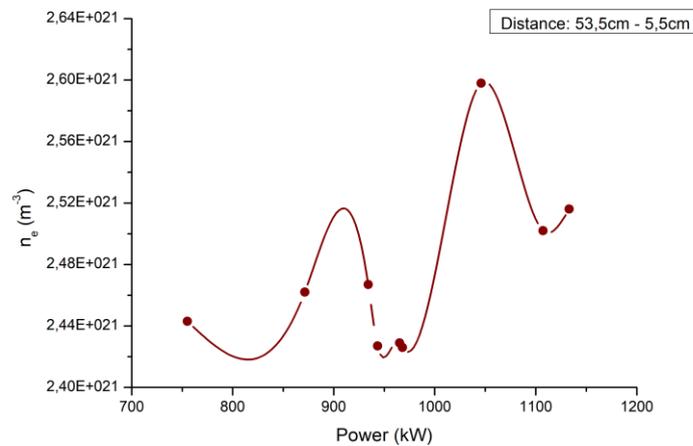**Figure 8: The alteration of T$_e$ with respect to the arc plasma power.**

Figure 9: The alteration of n$_e$ with respect to the arc plasma power.

Figure 10 displays the relationship between gas flow rate and T$_e$. The results show that electron temperature has dependence on the gas flow rate. The electron temperature, firstly, increased to 116 g/sec, then decreased to 119 g/sec and reached its maximum at 120 g/sec and decreased again. These decreases and increases in the electron temperature can be explained by the changes in the optical spectrometer distance. Even though the gas flow increases, the electron temperature is reduced when the optical spectrometer is moved away.
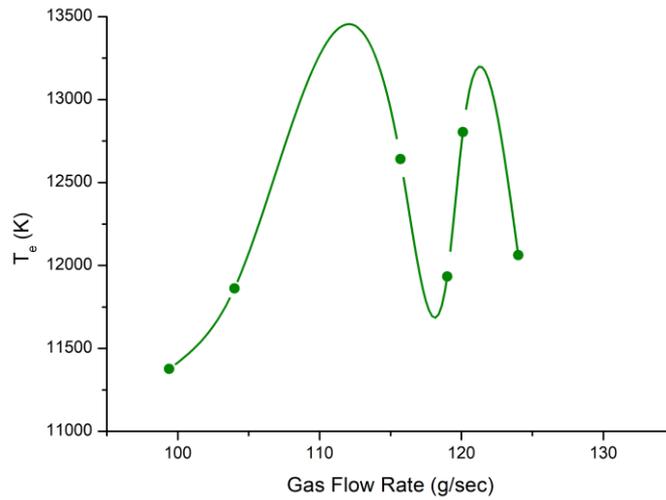
Figure 10: The alteration of T_e with respect to the gas flow rate.

According to Figure 11 which shows the evaluation of electron temperature with respect to the current it can be said that T_e increases with increased current. Therefore, the electron temperature is significant dependence on the current.
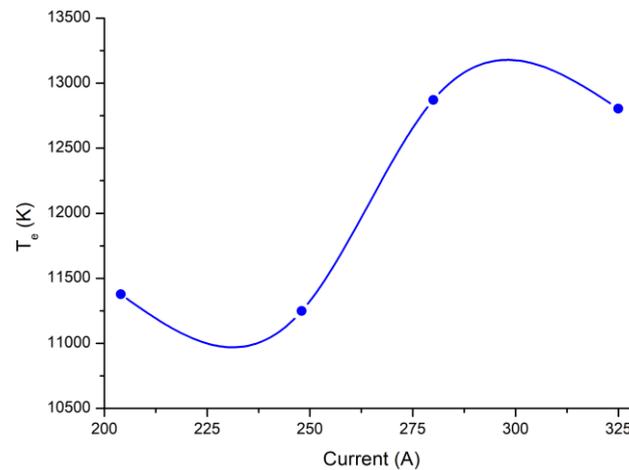
Figure 11: The evaluation of T_e with respect to the current.

With respect to theTable 2, all tests were performed with different modes which varied by the arc voltage, the arc current, the gas flow rate, the power and the chamber temperature. According to these variables and the position of optical spectrometer, the electron temperature and the electron density values are given in Table 2. Furthermore, the heat flux values which changes depending on the place of the probe were calculated by measuring flow rate and temperature differences of the cooling water using Equation 5. In addition, the gas flow rates were calculated using Equation 6 and chamber temperatures were calculated by Equation 7, explained above. These calculated values are also given inTable 2.

Table 2: Characteristics of the Plasmatron.

No	Distance of optical spectrometry [cm]	Test duration [sec]	Impedance Value (Ω)	I [A]	G_g [g/sec]	W [kW]	T_{ch} [K]	HF [MW/m²]	T_e [K]	n_e [m⁻³]
1	53.5 cm − 22 cm − 5.5 cm	30	27.5	204	82.8	664.8	4016	1.14	12755	2.587E+21
2	53,5 cm - 22 cm - 5,5 cm	25	27.5	204	118.9	713.38	4005	1	11933	2.503E+21
3	53.5 cm − 22 cm − 5.5 cm	25	27.5	204	93.6	732.4	3948	0.99	11668	2.474E+21
4	53.5 cm − 5.5 cm	25	27.5	204	99.4	755.2	3882	1.58	11376	2.443E+21
5	53.5 cm − 28.5 cm − 5.5 cm	25	27.5	204	115.6	839.9	3853	3.42	12034	2.513E+21
6	53.5 cm − 28 cm − 5.5 cm	25	27.5	204	115.7	861.8	3835	3.39	12642	2.575E+21
7	53.5 cm − 28 cm − 5.5 cm	25	27.5	204	123.7	869.8	3820	1.47	11919	2.501E+21
8	53.5 cm − 5.5 cm	25	22.5	248	104.9	871.3	4052	1.44	11547	2.462E+21
9	53.5 cm − 5.5 cm	25	22.5	248	114.9	934.14	4031	1.49	11574	2.467E+21
10	53.5 cm − 5.5 cm	25	22.5	248	112.7	943.4	4036	3.38	11223	2.427E+21
11	53.5 cm − 5.5 cm	25	22.5	248	120.4	965.3	3887	3.55	11248	2.429E+21
12	53.5 cm − 5.5 cm	25	22.5	248	118.3	968.1	4048	1.51	11211	2.426E+21
13	53.5 cm − 5.5 cm	25	20	280	117	1045.9	4226	2.38	12870	2.598E+21
14	30 cm − 5 cm	35	17.5	325	104	1022.6	4398	1.72	11709	2.479E+21
15	53.5 cm − 6 cm	15	17.5	325	115	1057.9	4345	3.38	11947	2.504E+21
16	53.5 cm − 6 cm	15	17.5	325	120	1074.1	4249	3.35	11962	2.506E+21
17	53.5 cm − 10 cm	25	17.5	325	116	1082.1	4269	2.01	12422	2.553E+21
18	30 cm − 5 cm	35	17.5	325	120.1	1094.8	4515	2.55	12804	2.495E+21
19	53.5 cm − 10 cm	25	17.5	325	121	1114.5	4198	1.65	12240	2.535E+21
20	53.5 cm − 10 cm	10	17.5	325	124	1117	4189	3.46	12532	2.565E+21
21	53.5 cm − 6 cm	15	17.5	325	126	1128.6	4520	3.34	12723	2.584E+21
22	53.5 cm − 5.5 cm	25	17.5	325	119	1107.2	4216	4.44	11933	2.502E+21
23	53.5 cm − 5.5 cm	25	17.5	325	124	1133.1	4204	5.05	12062	2.516E+21

I – average arc current; G_g – gas flow rate; W – power; T_{ch} – chamber temperature; HF – heat flux value; T_e – electron temperature; n_e – electron density.

V. CONCLUSION

Due to its wide range applications (energy, aerospace technologies, spraying of materials, chemical analysis, gas treatment, semiconductor production, gasification and combustion processes etc. [26]), plasma technology has been preferred and it requires an adequate analysis and characterization in order to enhance the efficiency of these applications. This paper shows the progress in experimental studies on the characterization of plasma by determining its physical parameters using the optical emission spectroscopy. To determine the electron temperature and electron density, the local thermal equilibrium is used since it is applicable for the atmospheric thermal plasmas. For this purpose, the experiments were made at different OES distances and different power values. O, N, N_2, O_2, CO and NO, OH radicals were observed in the measurements made with OES and the values of singly ionized nitrogen ions, NII, at 510.44 nm, 589.32 nm, 606.67 nm and 616.8 nm wavelengths were used in the calculations. The Boltzmann plot and McWhirter criterion were used to calculate the electron temperature and electron density, respectively. While the power changes from 750 kW to 1100 kW, the electron temperature is between 11248 K and 12870 K and the electron density changes from 2.429×10^{21} m⁻³ to 2.587×10^{21} m⁻³. In an inductively coupled plasma torch operating at 50 kW at atmospheric pressure, T_e and n_e were obtained as 11600 K and 1.0×10^{21} m⁻³ respectively with OES using LTE method [18]. In another study of

an atmospheric pressure plasma jet, T_e and n_e were calculated as 1.0 eV and 4.3×10^{22} m^{-3}, respectively [26]. Considering these similar studies in the literature, the plasma electron temperature and electron density in this study are evaluated at the expected levels. There is a relationship between power and plasma parameters. The dependency of T_e and n_e to the plasma power was observed with an increase at the lower power, and a decrease at higher power levels, having a maximum point. As maximum point for both plasma parameters (T_e and n_e) 1050 kW power level was observed,and this was thought thatuntil maximum level of the power, the energy is transmitted to the free electrons and so they gain more energy increasingT_e and n_e. Then, the values of T_e and n_e decreased, this was concluded that the electrons have started to transfer some part of their energy to the other heavy particles (ions and neutrals), causing a decreaseT_e and n_e, this results are consistent with our previous experimental results[14]. In this paper, the experimental studies of heat flux and chamber temperature were also given. Maximum chamber temperature and heat flux values could be obtained as 4515.3 K and 5.05 MW/m^2, respectively by adjusting operation conditions especially higher working flow gas rate (124 g/s), higher power (1133.1 kW).

REFERENCES

[1]. Tendero C., Tixier C., Tristant P., Desmaison J., Leprince P., Atmospheric pressure plasmas: A review,Spectrochimica Acta Part B 61 2 – 30 (2006).

[2]. Toraman S, Katırcıoğlu T. Y., Terzi Ç., The High-Power Arc-Jet Plasma Generator (Plasma Torch) Characteristics and Performance,International Journal of Engineering Technology and Scientific Innovation, ISSN: 2456-1851, Volume:02, Issue: 04, pp.680-699 (2017).

[3]. Ley H. H., Yahaya A., Raja Ibrahim R. K., Analytical Methods in Plasma Diagnostic by Optical Emission Spectroscopy: A Tutorial Review,Journal of Science and Technology, ISSN: 2229-8460, Vol 6, No 1 (2014).

[4]. Bogaerts A., Neyts E., Gijbels R, Mullen J., Gas Discharge Plasmas and Their Applications,Spectrochimica Acta Part B 57 609-658 (2002).

[5]. Ricard A, Plasmas reactifs, Edition SFV, Paris, 117 pp (1995).

[6]. FromNationalResearchCouncilDecadalReview, PlasmaScience: FromFundamentalResearchtoTechnological Applications (1995) http://www.nap.edu/catalog.php?record_id=4936 .

[7]. Devia D. M., L. V. Rodriguez-Restrepo, E. Restrepo-Parra, Methods Employed in Optical Emission Spectroscopy Analysis: a Review, PACS: 52.25.Dg, 31.15.V-doi:10.17230/ingciencia.11.21.12.

[8]. Donné A.J.H., Introduction to Plasma Diagnostics, Fusion Science and Technology, 53:2T, 379-386, (2008) DOI: 10.13182/FST08-A1723

[9]. Auciello O., Flamm D.L., Plasma Diagnostics, Vol.1. Discharge parameters and chemistry

[10]. Held M, Wharton C. Plasma Diagnostics with Microwaves, Wiley (1965).

[11]. Luhmanh N. C., Bindslev H., Park H., Sanchez J., Taylor G., Yu C. X., Microwave Diagnostics, (2007).

[12]. DONNÉ A.J.H., Diagnostics for Fluctuation Measurements, Transact. Fusion Sci. Techn. 49, 2T, 367 (2006).

[13]. Bings N. H.,. Bogaerts A, Broekaert J. A. C., Atomic Spectroscopy, Analytical Chemistry, p. 4317–4347, 240 (2008).

[14]. Yazıcıoğlu Ö, Katırcıoğlu T. Y., Güngör Ü. E., Spectroscopic and diagnostic analysis of a high-power AC plasmatron, International Journal of Current Research, 9 (10), 59757-59761.

[15]. Numano M., Criteria for local thermodynamic equilibrium distributions of populations of excited atoms in a plasma," Journal of Quantitative Spectroscopy & Radiative Transfer, pp. 311–317, 245 (1990).

[16]. Aragon C., Aguilera J. A., Characterization of laser induced plasmas by optical emission spectroscopy: A review of experiments and methods, Spectrochimica Acta Part B 63 893-916 (2008).

[17]. R. McWhirter, Plasma Diagnostic Techniques. Academic Press, 245 (1965).

[18]. Laux, C. O., Spence, T. G., Kruger C. H. and Zare, R. N., Optical diagnostics of atmospheric pressure air plasmas, Plasma Sources Sci. Technol. 12 125-138 (2003).

[19]. D. Haar, Elements of Statistical Mechanics. Elsevier Science, (1995). [Online]. Available: http://books.google.com.co/books?id=dt8GkhAgd88C 243

[20]. Hotinceanu M., Borsos Z, Dinu O., Aspects of Thermodynamic Equlibrium in Plasma,BuletinulUniversitatii Petrol – Gaze din Ploieşti, Vol. LXII No. 1/2010 97-102 SeriaMatematica – Informatica – Fizica

[21]. Kolpakova A., Kudrna P., Tichy M., Study of Plasma System by OES (Optical Emission Spectroscopy), ISBN 978-80-7378-185-9 WDS'11 Proceedings of Contributed Papers, Part II, 180-185, (2011).

[22]. Bottin, B., Chazot, O., Carbonaro, V., Van Der Heagen, V., Paris, S. The VKI plasmatron characteristics and performance. North Atlantic Treaty Organization (1999).

[23]. Zhukov, M. F.,Zasypkin, I. M. Thermal plasma torches design, characteristics, applications. Cambridge International Science Publishing 399-410 (2007).

[24]. Zhi S.X., Ping Y., Ming Z. H., JieW., Transition probabilities for NII 2p4f–2p3d and 2s2p23d–2s2p23p obtained by a semiclassical Method", IOPscience, no:10, (2007): 2934-2936.

[25]. NIST, NationalInstitute of StandardsandTechnology, 2018. https://www.nist.gov/pml/atomic-spectra-

[26]. Katırcıoğlu T. Y., Toraman S., Terzi Ç.,Review on theNeed of a MoreEfficient Three-Phase AC PlasmaCombustion/GasificationSystemforAll Solid WasteIncludingHazardousandBiomass, International Journal of EngineeringResearchand Applications, ISSN: 2248-6922, Vol.7 – Issue 10 (2017).

[27]. Förster S., Mohr C., Viöl W., Investigations of an atmosphericpressureplasma jet byopticalemissionspectroscopy, Elsevier, Surface&CoatingsTechnology, 200, 827830 (2005).

T. Yaşar Katırcıoğlu" Further Characteristic Analysis of the High-Power AC Plasmatron"International Journal Of Engineering Research And Development , vol. 15, no. 3, 2019, pp.29-39.